

An experimental study on creep deformation of thin-walled tubes under pure bending

Chien-Min Hsu†

Department of Arts-Craft, Tung Fung Junior College of Technology, Kao Hsiung County, Taiwan, R.O.C.

Chun-Huei Fan‡

Department of Engineering Science, National Cheng Kung University, Tainan, Taiwan, R.O.C.

Abstract. The creep deformation of pure bending (hold constant moment for a period of time) tests were conducted in this paper. Thin-walled tubes of 304 stainless steel were used in this investigation. The curvature-ovalization measurement apparatus, designed by Pan *et al.* (1998), was used for conducting the present experiments. It has been found that as soon as the creep deformation is started, the magnitudes of the tube curvature and ovalization of tube cross-section quickly increase. The magnitudes of the creep curvature and ovalization of tube cross-section increase fast with a higher hold moment than that with a lower one. Owing to the continuously increasing curvature during the creep deformation, the tube specimen buckles eventually.

Key words: thin-walled tube; pure bending; creep deformation.

1. Introduction

Many industrial components, such as offshore pipelines, platforms in offshore deep water, nuclear reactors, etc., are thin-walled tubes. Generally, they are subjected to the loading condition of pure bending. Therefore, proper understanding of the response of thin-walled tubes subjected to pure bending is of importance in many industrial applications. It has been found that the deformation characteristics of nonlinear moment-curvature relationship are well known and ovalization of the tube cross-section is also known to occur when the tube component is bent into plastic range. The magnitude of tube ovalization increases when the magnitude of the bending moment increases. Such increase in ovalization of tube cross-section causes a progressive reduction in its bending rigidity (accumulation of damage) which can ultimately result in buckling of the tube (Fabian 1977, Reddy 1979, Gellin 1980).

Studies have been made on circular tubes subjected to monotonic or cyclic pure bending with or without external pressure by Kyriakides and his co-workers. Kyriakides and Shaw (1982) designed a bending device that can be used for conducting the experiment on circular tubes subjected to cyclic bending. The magnitudes of bending moment and tube curvature can thus be measured. For the measurement of ovalization of the tube cross-section, Kyriakides and Shaw

† Instructor

‡ Graduate Student

(1983) designed a lightweight instrument which can be placed at the mid-span of the test specimen for measuring the ovalization of tube cross-section. The inelastic behavior of thin-walled tubes under cyclic bending were studied by them. These bending test facilities have been used for the subsequent experimental studies, for example, Shaw and Kyriakides (1985) investigated the inelastic buckling of tubes under cyclic bending; Kyriakides and Shaw (1987) performed an experimental investigations on the response and stability of thin-walled tubes under cyclic bending; Corona and Kyriakides (1988) studied the stability of long metal tubes subjected to combined bending and external pressure; Corona and Kyriakides (1991) discussed the degradation and buckling of circular tubes under cyclic bending and external pressure; and Kyriakides and Ju (1992) experimentally investigated the bifurcation and localization instabilities in circular cylindrical shells under pure bending.

In recent years, Pan and his co-workers have investigated experimentally and theoretically on the response and stability of circular tubes subjected to monotonic or cyclic bending. Pan *et al.* (1998) designed a new measurement apparatus, which can be placed at the mid-span of the circular tube specimen and is suitable for simultaneous experimental determinations of the tube curvature and ovalization of the tube cross-section. For testing the newly designed apparatus, the tube specimen of 304 stainless steel was cyclically bent. Pan and Hsu (1999) experimentally and theoretically studied the viscoplastic behavior of 304 stainless steel tubes subjected cyclic bending. The endochronic viscoplastic theory, which was proposed by Pan and Chern (1997), was used to investigate the viscoplastic behavior of the tubes under cyclic bending. Furthermore, Pan and Her (1998) used the aforementioned new measurement apparatus to investigate the response and stability of 304 stainless steel tubes subjected to cyclic bending with different curvature-rates. They discovered that the higher the applied curvature-rate, the greater is the degree of hardening of metal tube. However, the ovalization of tube cross-section increases when the applied curvature-rate increases.

In this paper, the creep deformation (hold constant moment for a period of time) of thin-walled tubes under pure bending was studied. A four-point bending machine (Pan *et al.* 1998, Pan and Hsu 1999, Pan and Her 1998) was used for conducting the pure bending tests. The material of the thin-walled tube chosen for this study was 304 stainless steel. The curvature-ovalization measurement apparatus (COMA), designed by Pan *et al.* (1998), was used. The creep deformation was controlled by the load cell. The magnitudes of curvature and ovalization of the tube cross-section were simultaneously measured by the COMA. The magnitude of the bending moment was obtained from the two load cells, mounted in the bending machine. It was observed from the experimental result that based on the variation of the tube curvature-time curve, the creep process can be divided into two stages, the initial creep and the steady-state creep stages. Once the creep deformation is started the magnitude of the tube curvature quickly increases (the initial creep stage). But thereafter, the tube enters steady-state creep stage, and the curvature increases steadily with time. It was found that the larger magnitude of the hold moment, the faster the tube curvature increases. Furthermore, the ovalization of tube cross-section increases steadily in the initial creep stage, however, the ovalization increases quickly with time in the steady-state creep stage. Due to the continuously increasing curvature during the creep deformation, the tube specimen buckles finally.

2. Experimental facilities

In this study, a bending test facility was used to carry out a number of experiments on thin-walled tubes under creep deformation. The facility consists of a pure bending device and a curvature-ovalization measurement apparatus (COMA). Further description of the test facility is made in the following.

2.1. Bending device

Fig. 1(a) shows a schematic drawing of the bending device, and Fig. 1(b) shows a picture of the bending device. It was designed as a four-point bending machine, capable of applying bending. The device consists of two rotating sprockets, about 30 cm in diameter, symmetrically resting on two support beams of 1.25 m apart. The maximum length of the test specimen allowed is 1 m. The two sprockets support two rollers which apply point loads in the form of a couple at each end of the test specimen. Heavy chains run around these sprockets and are connected to two hydraulic cylinders and load cells forming a closed loop. Once either the top or bottom cylinder contracts, the sprockets rotate, and pure bending of the test specimen is achieved. The contact between the tube and the rollers is free to move along axial direction during bending. The load transfer to the test specimen is in the form of a couple formed by concentrated loads from the two rollers. Detailed description of such a bending device can be found in literature (Pan *et al.* 1998, Pan and Her 1998, Pan and Hsu 1999).

2.2. Curvature-ovalization measurement apparatus (COMA)

The curvature-ovalization measurement apparatus (COMA), as shown in Fig. 2(a), is a lightweight instrument, mounted close to the tube's mid-span (Pan *et al.* 1998). A picture of the COMA used in

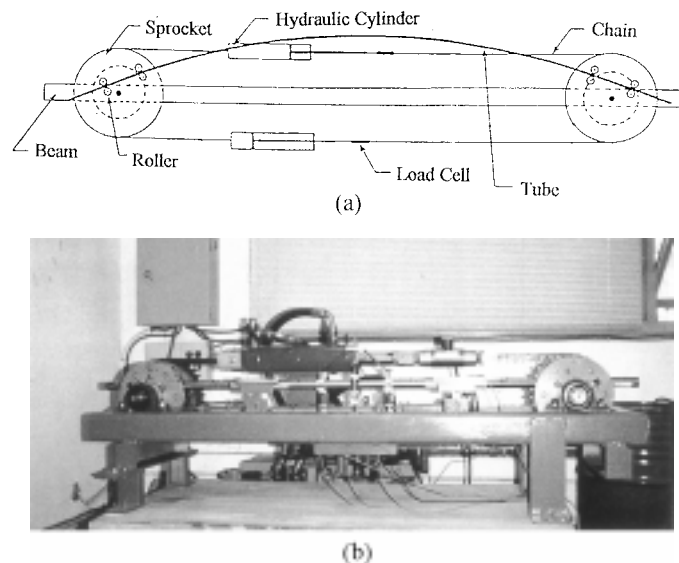


Fig. 1 (a) Schematic drawing of the bending device, (b) a picture of the bending device

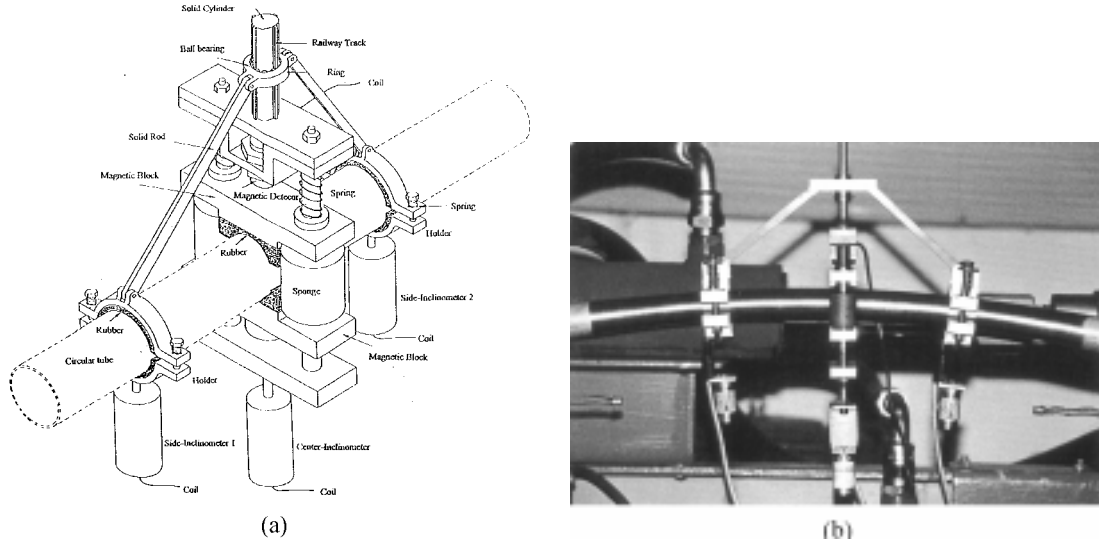


Fig. 2 (a) Schematic drawing of the COMA, (b) a picture of the COMA

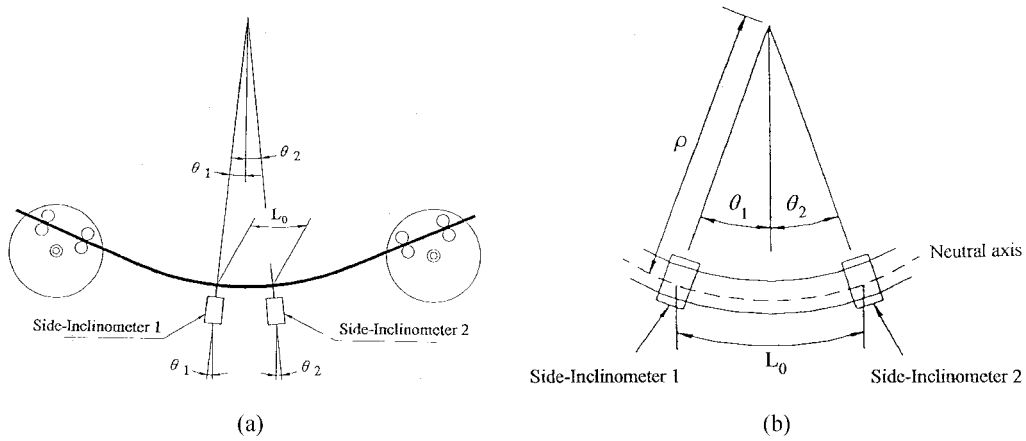


Fig. 3 (a) Angle changes measured by two side-inclinometers under pure bending, (b) deformation between two side-inclinometers

this study is shown in Fig. 2(b). Using a magnetic detector (middle part of the COMA), it can monitor the changes in the major and minor diameters of the tube cross-section (the ovalization of tube cross-section). Simultaneously, it can measure variations in the tube curvature close to the mid-span from the signals of two side-inclinometers (see Fig. 2a). Based on the fixed distance between the two side-inclinometers (L_0) and the angle changes detected by the two side-inclinometers (θ_1 and θ_2), the tube curvature can be obtained as (Figs. 3a and 3b)

$$L_0 = \rho (\theta_1 + \theta_2) \tag{1}$$

where ρ is the distance between the center of this arc and the neutral surface. The curvature of the tube κ is

$$\kappa = \frac{1}{\rho} = \frac{(\theta_1 + \theta_2)}{L_o} \quad (2)$$

The angle of rotation detected by the center-inclinometer is in the plane, which is perpendicular to the plane of the bending moment. The center-inclinometer can be used for inspecting the deviation of the plane, in which the aforementioned two side-inclinometers are fixed, from the plane of the bending moment. Detail description of the COMA can be found in the work by Pan *et al.* (1998).

3. Experimental investigation

In this section, we discuss the specimens and the test procedures of creep deformation of thin-walled tubes subjected to pure bending. Specimens and the test procedures are given below:

3.1. Material and specimens

The material used in this study was SUS 304 stainless steel, with chemical composition: Cr 18.36, Ni 8.43, Mn 1.81, Si 0.39, C 0.05, P 0.28, S 0.004 and Fe remainder. To obtain the desired ratio of outside diameter D to wall thickness t (D/t), the tubes originally with $D=31.8$ mm and $t=1.5$ mm ($D/t=21.2$) were slightly machined on the outside surface. Fig. 4 shows the dimensions of the test specimen. The outside surfaces of all tested tubes are smooth. There is no local indentation on the outside surface. The outside diameter, wall thickness and gage length are 30.33, 0.76 and 388 mm, respectively, i.e. D/t is approximately equal to 40.

3.2. Test procedures

The bending test was conducted by using the bending device described in Section 2.1. The magnitude of the curvature was controlled and measured by the COMA which also measured the ovalization of tube cross-section. The bending moment can be calculated from the signals detected by the two load cells, mounted in the bending device.

For creep test, the specimen was bent in the curvature-controlled mode (controlled by the COMA) at the preloading stage while the computer monitored the magnitude of the moment. To avoid the viscoplastic behavior of 304 stainless steel tube (Pan and Her 1998), the speed of loading applied on the tube was very slow. As soon as the moment magnitude reached the preset creep hold moment, the loading process stopped. The test system was programmed to switch to the moment-controlled mode (controlled by the load cells) instantaneously and the moment was kept at this constant magnitude, while the tube curvature and ovalization of tube cross-section were being recorded.

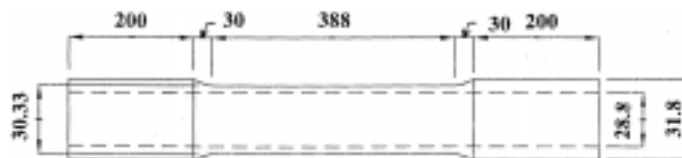


Fig. 4 Geometry of thin-walled tubular specimen (all dimensions in mm)

4. Results and discussion

In this section, the experimental data of thin-walled tubes for SUS 304 stainless steel under creep deformation are discussed. Note that the creep deformation is to hold a constant moment for a period of time.

4.1. Pre-creep stage

Fig. 5 presents the moment (M)-curvature (κ) curves of the thin-walled tubular specimen under pure bending at pre-creep stage. It can be seen that due to the deformation in the plastic range, the nonlinear moment-curvature curve is observed. Fig. 6 shows the corresponding ovalization of tube cross-section as a function of the applied curvature. The ovalization of tube cross-section is defined by $\Delta D/D$ where D is the outer diameter and ΔD is the change in outer diameter. It can be noted that the ovalization of tube cross-section increases when the applied curvature increases.

4.2. Creep stage

Fig. 7 depicts the curvature (κ)-time (t) profile of the whole loading process under pure bending (pre-creep and creep stages). The magnitude of the hold moment for creep stage is 150 N-m. The starting and buckling points of the creep stage are marked by “•” and “×”, respectively. It can be observed from Fig. 7 that the creep process can be divided into two stages, the initial creep and the steady-stage creep stages. It could be seen from Fig. 7 that as soon as the creep is started the magnitude of the tube curvature quickly increases (the initial creep stage). This stage is terminated in a short time. But thereafter, the tube enters steady-state creep stage, and the curvature increases steadily with time. Owing to the continuously increasing curvature at the creep deformation, the tube specimen buckles eventually. Fig. 8 demonstrates the ovalization ($\Delta D/D$)-time (t) profile of the whole loading process under pure bending at same hold moment of 150 N-m (pre-creep and creep stages). Note that the definition of the ovalization in creep stage is the same as the definition in pre-

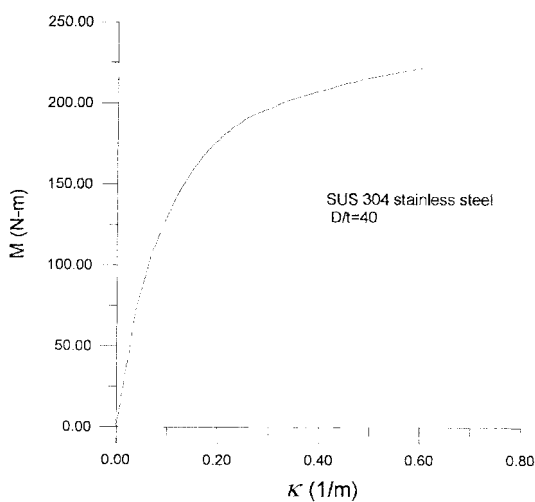


Fig. 5 Moment-curvature curve under pure bending

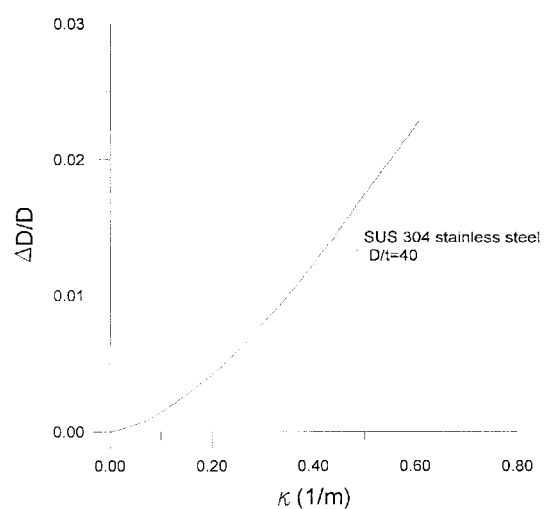


Fig. 6 Ovalization-curvature curve under pure bending

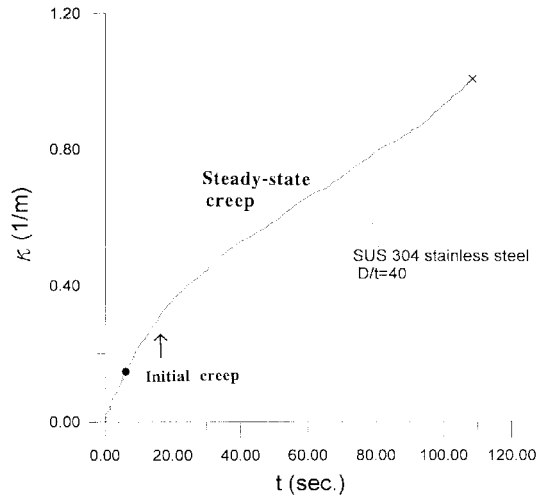


Fig. 7 Curvature-time curve under creep deformation with the hold moment of 150 N-m (“•” and “x” denote the starting and buckling points of the creep stage, respectively)

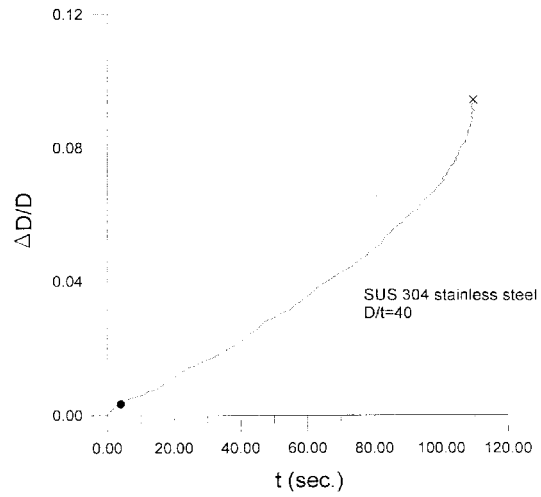


Fig. 8 Ovalization-time curve under creep deformation with the hold moment of 150 N-m (“•” and “x” denote the starting and buckling points of the creep stage, respectively)

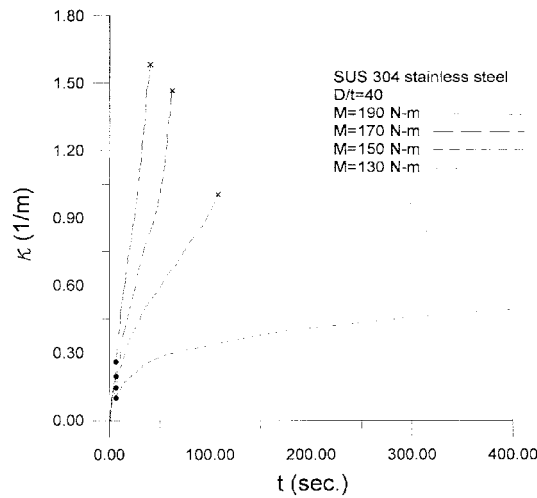


Fig. 9 Curvature-time curves under creep deformation with four different magnitudes of hold moment (“•” and “x” denote the starting and buckling points of the creep stage, respectively)

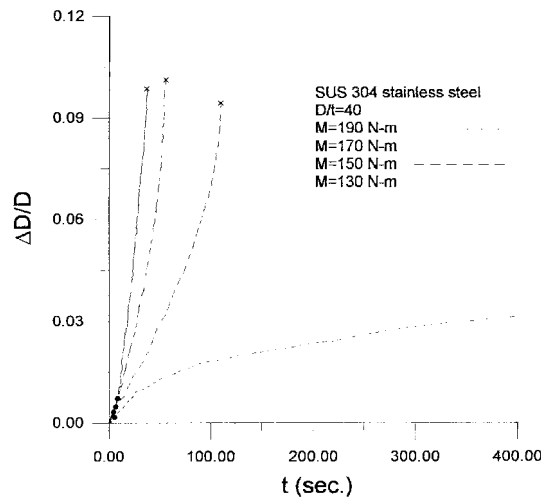


Fig. 10 Ovalization-time curves under creep deformation with four different magnitudes of hold moment (“•” and “x” denote the starting and buckling points of the creep stage, respectively)

creep stage shown in Sec. 4.1. The starting and buckling points of the creep stage are also marked by “•” and “x”, respectively. It has been shown that the ovalization of tube cross-section increases steadily at the initial creep stage, however, the ovalization of tube cross-section increases quickly with time at the steady-state creep stage. Fig. 9 depicts the curvature-time profiles of the whole loading process under pure bending (the pre-creep and the creep stages). Four different magnitudes

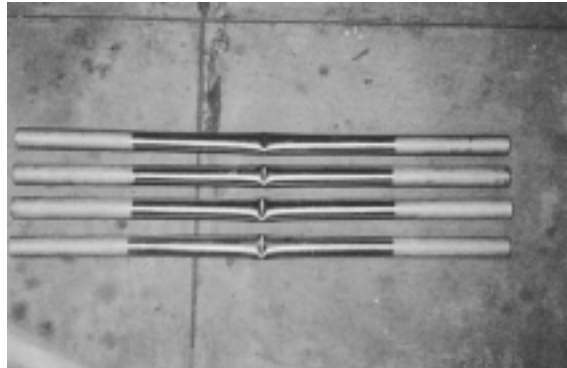


Fig. 11 Picture of the local buckling for 304 stainless steel tubes under pure bending creep

of the hold moment, i.e. 130, 150, 170 and 190 N-m, were controlled for tube specimens under creep deformation. It has been shown that the initial curvature-rate of the creep deformation with higher hold moment is large, and the corresponding creep curvature is larger than that of creep deformation with a smaller hold moment. Due to much longer time for buckling under hold moment of 130 N-m, the buckling point of the curvature-time curve does not indicate in Fig. 9. It can also be seen from Fig. 9 that the magnitudes of the creep curvature at buckling for these four hold moments are different. The curvature at buckling with a higher hold moment is larger than that with a smaller hold moment. The corresponding ovalization-time curves of the whole loading process under four different magnitudes of hold moment (the pre-creep stage and the creep stage) are demonstrated in Fig. 10. It can be observed that the initial ovalization-rate of the creep deformation with higher hold moment is large, and the corresponding ovalization is larger than that of creep deformation with a smaller hold moment. However, the ovalizations at buckling for these four magnitudes of hold moment are almost the same. It is noted that due to much longer time for buckling for hold moment of 130 N-m, the buckling point of the ovalization-time curve does not indicate in Fig. 10. Fig. 11 shows a picture of the local buckling of 304 stainless steel tubes under pure bending creep.

5. Conclusions

The creep deformation of thin-walled tubes under pure bending is investigated in this study. Four different hold moments were used to highlight the creep behavior of thin-walled tubular specimens for 304 stainless steel. The following important conclusions can be drawn from this investigation:

1) The creep process can be divided into two stages, the initial creep and the steady-state creep stage from the creep curvature curves. Once the creep deformation is started the magnitude of the tube curvature quickly increases (the initial creep stage). But thereafter, the tube enters steady-state creep stage, and the curvature increases steadily with time. The ovalization of tube cross-section increases steadily at the initial creep stage, however, the ovalization of tube cross-section increases quickly with time at the steady-state creep stage.

2) The creep curvature-rate is larger with a higher hold moment than that with a lower one. In addition, the magnitudes of creep curvature at buckling for these four holding moments are

different. The curvature at buckling with a higher hold moment is larger than that with a smaller hold moment.

3) The creep ovalization-rate of tube cross-section is larger with a higher hold moment than that with a lower one. However, the magnitudes of creep ovalization at buckling for these hold moments are almost the same.

Acknowledgements

The reported experimental work was carried out by using the bending facilities from Professor W. F. Pan (Department of Engineering Science, National Cheng Kung University). His support is gratefully acknowledged.

References

- Corona, E. and Kyriakides, S. (1988), "On the collapse of inelastic tubes under combined bending and pressure", *Int. J. Solids Struct.*, **24**(5), 505-553.
- Corona, E. and Kyriakides, S. (1991), "An experimental investigation of the degradation and buckling of circular tubes under cyclic bending and external pressure", *Thin-Walled Struct.*, **12**, 229-263.
- Fabian, O. (1977), "Collapse of cylindrical, elastic tube under combined bending, pressure and axial loads", *Int. J. Solids Struct.*, **13**, 1257-1273.
- Gellin, S. (1980), "The plastic buckling of long cylindrical shell under pure bending", *Int. J. Solids Struct.*, **16**, 397-407.
- Kyriakides, S. and Shaw, P.K. (1982), "Response and stability of elastoplastic circular pipes under combined bending and external pressure", *Int. J. Solids Struct.*, **18**(11), 957-973.
- Kyriakides, S. and Shaw, P.K. (1983), "Buckling of plastic tubes under cyclic bending", *Proc. 4th Eng. Mech. Div., ASCE Spec. Conf., Purdue University*, **I**, 604-667.
- Kyriakides, S. and Shaw, P.K. (1987), "Inelastic buckling of tubes under cyclic loads", *ASME J. Press.Vessel Technol.*, **109**, 169-178.
- Kyriakides, S. and Ju, G.T. (1992), "Bifurcation and localization instabilities in cylindrical shells under bending, I: Experiments", *Int. J. Solids Struct.*, **29**(9), 1117-1142.
- Pan, W.F. and Chern, C.H. (1997), "Endochronic description for viscoplastic behavior of materials under multiaxial loading", *Int. J. Solids Struct.*, **34**(17), 2131-2160.
- Pan, W.F. and Her, Y.S. (1998), "Viscoplastic collapse of thin-walled tubes under cyclic bending", *ASME J. Engng. Mat. Technol.*, **120**, 287-290.
- Pan, W.F., Wang, T.R. and Hsu, C.M. (1998), "A curvature-ovalization measurement apparatus for circular tubes under cyclic bending", *Experimental Mechanics*, **38**(2), 99-102.
- Pan, W.F. and Hsu, C.M. (1999), "Viscoplastic analysis of thin-walled tubes under cyclic bending", *Int. J. Struct. Engng. Mech.*, **7**(5), 457-471.
- Reddy, B.D. (1979), "An experimental study of the plastic buckling of circular cylinders in pure bending", *Int. J. Solids Struct.*, **15**, 669-683.
- Shaw, P.K. and Kyriakides, S. (1985), "Inelastic analysis of thin-walled tubes under cyclic bending", *Int. J. Solids Struct.*, **21**(11), 1073-1100.